Numerical Simulation of HSCT Inlet Operability with Angle of Attack

Ge-Cheng Zha* and Doyle Knight†
Dept. of Mechanical and Aerospace Engineering
Center of Computational Design
Rutgers University - The State University of New Jersey
PO Box 909 · Piscataway NJ 08855-0909

Donald Smith‡
Dept. of Computer Sciences
Center of Computational Design
Rutgers University - The State University of New Jersey
PO Box 909 · Piscataway NJ 08855-0909

Martin Haas§
United Technologies Research Center
East Hartford, Connecticut 06180

Abstract

A High Speed Civil Transport (HSCT) inlet at Mach 2 and angle of attack is simulated by using a 3D Navier-Stokes solver with the Baldwin-Lomax algebraic turbulence model. An extrapolation uniform mass bleed boundary condition for the slot bleed is successfully employed. For zero angle of attack and critical operation, the pressure distribution agrees well with the experiment. The location and intensity of the terminal shock, total pressure recovery are accurately computed. The angle of attack to cause the inlet unstart is accurately predicted. The mesh refinement results are presented.

* Research Associate, AIAA Member
† Professor, AIAA Associate Fellow
‡ Assistant Professor
§ Senior Research Engineer, AIAA Member

1 Introduction

The critical technologies required to develop a High Speed Civil Transport (HSCT) are being investigated in the United States and Europe. A high performance HSCT propulsion system and airframe is vital for the competition in the global HSCT market [1, 2]. The supersonic flight regime of HSCT results in issues which are not present for its subsonic counterpart. As an important component of the HSCT propulsion system, the HSCT inlet needs to work with high efficiency and a wide stability margin.

HSCT inlet unstart at cruise condition is an extremely important issue in the design of a HSCT inlet. For flight speed over Mach 2, mixed-compression inlets offer the capability to operate efficiently with low drag over the entire flight range. For high cruise efficiency, the mixed compression inlet is designed to operate at the so called "critical operation". The "critical operation" locates a terminal shock just downstream of the throat to maintain high total pressure recovery with the maximum mass flow. Such a flow condition is called inlet "start". However, the terminal shock location is very sensitive to

disturbance and can be pushed out of the inlet to cause the inlet "unstart". An inlet unstart would result in transient forces on the aircraft which would effect passenger comfort and safety and may also cause engine surge. The range of operating conditions (e.g., Mach number, angle of attack etc.) wherein the inlet remains started is known as the "operability" of the inlet.

The disturbance which can induce inlet unstart can be either a variation of upstream flight conditions or the corrected weight flow required by the compressor. To increase the inlet control operability, boundary layer bleed is usually employed in the region of the throat to resist the disturbance. The design of boundary layer bleed, such as the bleed location and bleed mass rate, is crucial to provide an HSCT inlet with high efficiency, broad stability margin and low drag. To design high performance boundary layer bleed, wind tunnel tests are necessary. However with more and more powerful computers, to reduce the design cycle and costs, CFD now is usually used to guide the design before the final test.

Nevertheless, using CFD to accurately simulate the HSCT inlet flow with boundary layer bleed is very challenging. For the NASA VDC inlet which is studied in this paper, Saunders and Keith [3] did the first CFD simulation with zero angle of attack by using an axisymmetric Navier-Stokes solver. They used two different types of bleed boundary conditions. One was to specify the velocity profile across the bleed slot region [4], the other was to use constant pressure across the bleed region and adjust the bleed mass flowrate to the required one incorporated in PARC code [5]. They indicated significant difficulties in computing the critical flow. They obtained the critical flow with either the back pressure reduced by about 18% from the experimental value or the cowl translated by 3%. They mainly attributed the computational difficulties to the bleed boundary conditions they used. Slater et al. [6] used the boundary conditions similar to the constant pressure boundary condition of the PARC code and computed the same inlet at zero angle of attack. The shock location was significantly displaced from the experimental position when the experimental back pressure of the critical flow was imposed.

For the operability of high speed mixed compression inlets, various numerical studies have been carried out focusing on different subjects. Mayer and Paynter [7, 8] used an Euler solver and simulated the inlet operability due to the variation of free stream variables such as temperature, velocity and pressure. Slater et al. [9, 6] simulated the unstart/restart due to the freestream disturbance with moving geometry. Neaves and McRae [10] used the dynamic solution-adaptive grid algorithm of Benson and McRae and simulated the 2D and 3D inlet unstart due to the freestream and compressor face perturbations. Goble et al. [11] used a 3D Euler code to simulate the unsteady flow of the F-22 inlet with the hammershock from the engine face. Miller and Smith conducted an Navier-Stokes simulation of 2D high speed inlet unstart due to the back pressure disturbance [12]. These studies made contributions from different aspects to investigate the high speed inlet operability with boundary layer bleed. However, most of the above results did not have experiments to be compared with and are not quantitative. Some comparison with experiment was given in [6]. But the shock location and profile were largely deviated from the experiment at the critical operation under the experimental back pressure. It therefore still limited their results at the qualitative level. These studies were all at zero angle of attack. Hence, for some of the cases, the computation benefited from the axisymmetry of the flow field to save CPU time.

For the numerical studies on high speed inlet operability due to the angle of attack with boundary layer bleed, no work has been reported. Vadyak et al. [13] made the first computation of the flow field of a mixed compression inlet with angle of attack using the method of characteristics with shock fitting. Due to their numerical solver limitation, they did not take into account the wall boundary layer and boundary layer bleed. They were thus not able to predict the inlet unstart due to the angle of attack. Howlett and Hunter [14] computed a 3D external compression inlet with angle of attack. The unstart was not a problem in their work and there was no boundary layer bleed in that inlet.

The purpose of the present work is to determine the capability using CFD to predict the

unstart angle of attack for a typical HSCT inlet. This work is the first computational effort to study the unstart of a mixed compression inlet with boundary layer bleed induced by the angle of attack. Accurate simulation of HSCT inlet operability due to angle of attack is very important to achieve a design of HSCT inlet with high efficiency and wide stability margin [15].

2 The Inlet

The inlet studied in this work is the NASA Variable Diameter Centerbody (VDC) inlet designed and tested in Lewis Research Center in 1975 as shown in Fig. 1 [16, 17, 18]. It is a bicone, mixed-compression inlet with design cruise Mach number 2.5. A two-cone spike was used to provide the maximum external compression compatible with high total pressure recovery and relatively low cowl drag. In order to vary the contraction ratio for a flight inlet, the angle of the second cone could vary, and at its lowest position it would blend into the first-cone contours so as to provide a single-cone centerbody. This structure provides 45% of the supersonic area contraction internally for a design Mach number of 2.5. The inlet was designed such that the isentropic compression from the cowl and the cowl-lip oblique shock were nearly focused on the inlet's centerbody. A centerbody bleed slot was provided over this compression region for boundary layer control just ahead of the inlet throat. The inlet was tested at Mach number of 2.5 and 2. At Mach 2.5 at the critical operation, the maximum total pressure recovery with only 0.02 centerbody bleed mass-flow ratio and no cowl bleed was 0.906. The bleed mass-flow ratio is the ratio of bleed mass flow rate to the captured mass flow rate of the inlet. At Mach 2, the inlet total pressure recovery was 0.938 with only 0.013 centerbody bleed mass-flow ratio at critical operation. The experiment provided the data for the maximum angles of attack at which the inlets remain started for both Mach numbers and geometries. In this study, we examine the Mach 2 case which had a sealed downstream bypass door so that the computation can be more easily implemented. For the Mach 2 geometry, the initial cone angle was 12.5° and the second cone angle was 14.5°.

3 Numerical Procedures

3.1 Flow Solver and Mesh

To simulate the HSCT inlet operability, accurate prediction of the following physical phenomena are critical: 1) wall boundary layer development, 2) boundary layer bleed, 3) shock quality (shock intensity and propagation speed), 4) shock wave/turbulent boundary layer interaction. To meet the above physical needs, the following numerical procedure and boundary conditions were used.

The GASP code [19] was used as the CFD solver to compute the flow field. The Reynolds-averaged 3D compressible time dependent Navier-Stokes equations were solved. The Baldwin-Lomax algebraic turbulence model was used to simulate turbulence. Both the Roe and Van Leer upwind scheme were used in our computation to evaluate the convective and pressure terms. The Roe scheme was only able to compute the axisymmetric flow and failed in 3D flow due to an anomalous solution. The Van Leer scheme was satisfactory for all flows. The other important merit of Van Leer scheme was that the allowable CFL was 18 which was about 5 times higher than that of the Roe scheme. This was important since multiple flowfield simulations were required at different angle of attack and downstream pressure. Central differencing was used for the viscous terms. The MUCSL type differencing with Min-Mod limiter was used to evaluate the interface variables. The time integration method was the hybrid AF/Relaxation one which solved the implicit operator using approximate factorization (AF) in the spanwise plane and relaxation sweeping in the streamwise direction. One streamwise sweep per time step and no inner iteration was used. The initial flow field was generated from the uniform freestream flow with the mesh sequencing technique.

Fig. 2 is the 3D mesh used for the NASA VDC inlet [16] with 201 points in streamwise direction, 31 points in circumferential direction and 81 points in radial direction. The narrow band before the inlet throat with dense mesh in the streamwise direction is the boundary layer bleed region. Table 1 and 2 show the flow conditions

Table 1: Flow Conditions

Parameter	*Value*
M_∞	2.0
$P_{t\infty}$	7.67×10^4 Pa
$T_{t\infty}$	$390^o K$
Reynolds No.	6.54×10^6 /m
bleed mass/captured mass	1.3%

and mesh conditions respectively.

The axisymmetric baseline case has the same mesh size as that in a plane of the baseline 3D mesh as shown in Table 2. One of the purposes of the axisymmetric computation is to verify if the circumferential mesh size is sufficient for the 3D computation. Since the computational cells are represented by straight line segments, the mesh point distribution in circumferential direction must be sufficient to provide the correct capture mass flow rate. The operability of HSCT inlet is mass flow rate sensitive. The error of the circumferential area representation should be sufficiently small so that it has no significant influence on the inlet operability. Fig. 4 indicates that the circumferential mesh point is adequate since the pressure distributions predicted by the axisymmetric and 3D mesh are almost identical.

A bi-section root search iteration is used to find the proper back pressure corresponding to the critical operation [20]. The computation of the axisymmetric computation is much more efficient than the 3D one. Therefore the second function of the axisymmetric computation is to help the 3D computation search the back pressure corresponding to the critical operation. The turn-round CPU time of the 3D computation for one back pressure search varies from about 2 days to 20 days on single SGI Power Onyx R10000 processor. The higher the back pressure, the faster the shock moves, and therefore, the less is the CPU time needed to identify if the inlet starts or not. We benefited from multiple (3) processors by submitting multiple jobs in parallel.

Bi-section method was also used to search the unstart angle of attack. The turn-round CPU time for one search varies from 3 days to 20 days on a SGI Power Onyx R10000 processor corresponding to different angle of attack.

As we mentioned above, the Roe scheme for the axisymmetric case computation worked very well. However, moving the computation of the zero attack angle case from the axisymmetric domain to 3D brought a lot of difficulties using the Roe scheme. The computation started with supercritical flow using the extrapolation downstream boundary conditions. There was no terminal shock in the region of the throat for the supercritical flow and the Roe scheme performed well for this case. We then imposed the back pressure and gradually forced the terminal shock to the throat. With the terminal shock approaching the throat, Roe's scheme created an anomalous solution upstream of the throat. Fig. 3 demonstrates the circumferential Mach number contours upstream of the throat. The correct solution should have no circumferential gradient since the flow has zero angle of attack. However, the Roe scheme produced two low speed bulges at about $\pm 45°$. The low speed bulges seriously block the mass flow and the computation never obtained the started flow for 3D case using the Roe scheme. Harten's entropy fix [21] was used and smeared the two bulges. However, there was still strong circumferential gradient and always caused the inlet unstart. The Van Leer scheme worked excellently for all the cases with no circumferential gradient and therefore was chosen for all the 3D computation in this work.

3.2 Boundary Conditions

The upstream boundary condition used fixed variables equal to those of freestream. The no-slip conditions were used for the solid wall. First order extrapolation was used for the outer boundary upstream of the cowl leading edge. This boundary condition worked well to avoid the wave reflection and therefore the computation of the outer zone of the inlet was omitted to save the CPU time. At the subsonic outflow, the constant back pressure boundary condition was used and all other variables were first order extrapolated. The back pressure was fixed for each back pressure search iteration and altered by the bi-section rule until the terminal shock location agreed with the experiment. It is therefore an accuracy as-

Table 2: Grid Parameters

Parameters	*3D*	*Baseline Axisymmetric*	*Refined Axisymmetric*
grid points in streamwise	201	201	401
grid points in radial	81	81	161
grid points in circumferential	31	2	2
$\Delta x/\delta_{throat}$	0.3	0.3	0.15
$\Delta r^+_{1\ max,centerbody}$	2.3	2.3	0.98
$\Delta r^+_{1\ ave,centerbody}$	1.3	1.3	0.6
$\Delta r^+_{1\ max,cowl}$	1.9	1.9	0.8
$\Delta r^+_{1\ ave,cowl}$	1.1	1.1	0.5
grid points within both BL_{throat}	33	33	65
grid cells within bleed region	12	12	24

sessment criterion to compare if the back pressure searched agrees well with the experiment.

The bleed boundary condition was first order extrapolation for all the variables except for the normal velocity which was determined based on uniform bleed mass flowrate. This boundary condition was a reasonable approximation to the slot bleed used in the experiment. Our numerical tests showed that this bleed boundary condition was robust. The current bleed boundary condition is similar to the BC type 5 suggested by Chyu et al.[22]. The difference is that we do not not use the momentum equation to solve the pressure. We found that the momentum equation was not easily simplified and introduced numerical instability. In addition, we impose the first order derivative of the tangential velocity to be zero instead of the second order derivative to be zero as in [22]. The present bleed boundary condition was incorporated into the GASP code by the authors.

4 Mesh Refinement Computation

Mesh refinement computation is needed to access the accuracy and uncertainty of the computation using the baseline mesh. As mentioned above, the 3D computation is very expensive. The complete 3D mesh refinement test is too CPU intensive to proceed particularly due to the root search for the back pressure and the angle of attack. We therefore have to select a case with the most basic physical impacts on the flow field to carry out the mesh refinement study.

As we mentioned above, we verified that the circumferential mesh size might be sufficient by comparing the results with the axisymmetric case as shown in Fig. 4. We tend to believe that the same conclusion applies even with the angle of attack because the angle of attack under investigation is not large. Hence the flow variable gradient in the circumferential direction is far less than those in the streamwise and radial direction.

The case which we chose for the mesh refinement test and we considered as critical was the axisymmetric case with zero angle of attack. The mesh is then refined in both axial and radial direction. The refined mesh will enhance the resolution of the wall boundary layer, oblique and normal shock wave system and thus the shock wave/turbulent boundary layer interaction. All these physical phenomena are crucial to determine the inlet oparability, i.e., start or unstart. If the result of the axisymmetric case with zero angle of attack is converged based on the mesh refinement, we therefore may have sufficient confidence to believe that the 3D results of the baseline case will also not be sensitive to the refined mesh, in particular, from the inlet operability point of view.

Table 2 shows the grid resolution of the refined mesh with the size of 401x161 in streamwise and radial directions, respectively. Fig. 4 shows the

pressure distribution computed using the refined mesh for the axisymmetric case with zero angle of attack. The result is nearly identical to the baseline one. Fig. 4 also indicated that the shock location and intensity predicted by the refined mesh is the same as that of the baseline case. The back pressure searched for the axisymmetric refined mesh to keep the inlet started at the critical operation is 0.17% lower than that of the axisymmetric base line case. The back pressure difference of the 3D and the refined axisymmetric computation is 0.4%. The total pressure recovery is predicted to be 0.945 for the axi. The baseline axisymmetric case predicted the total pressure recovery to be 0.95 and the baseline 3D case predicted to be 0.939. The total pressure recovery of the refined mesh is in the middle of the results of the baseline axisymmetric and 3D case and the difference is within 0.7%. These results may conclude that the mesh size of the baseline case is sufficient to resolve the boundary layer and shock waves.

5 Results and Discussion

5.1 Zero Angle of Attack

The zero angle of attack flow is necessary as the initial flow field to compute the flow with angle of attack. It also has the detailed experimental results which can be used to assess the accuracy of the computation.

Fig. 4 displays the pressure distributions (normalized by the freestream total pressure) compared with the experiment [16] at zero angle of attack ($\alpha = 0.0°$) and critical operation. The experimental bleed mass rate of 1.3% is used and the computation is done in the axisymmetric and 3D domains. The back pressure searched from the axisymmetric and 3D case deviate from the experiment by 2.5% and 1.8%, respectively, which is comparable to the experimental uncertainty. The shock location and intensity match the experiment very well. However, there is a pressure oscillation before the normal shock which is considered to be introduced numerically due to the shock interaction with the bleed boundary condition. This oscillation is acceptable and is a minor side effect compared with the overall good agreement of the shock location and shock intensity. The computed pressure also agrees very well with the experiment upstream and downstream of the shock. However, there is a region downstream of $x/R_c = 4.2$ in the subsonic diffuser where the computation and experiment deviate, where R_c is the cowl radius of the inlet. One possible reason for the deviation is that there might be a flow separation in that region in the wind tunnel test. However, the experiment reported no separation in the portion of the subsonic diffuser. The present computation also predicted no separation. The other possible reason may be the following: in the experiment, vortex generators were installed to eliminate the flow separation in the subsonic diffuser. The difference in axial pressure distribution in the subsonic diffuser could be due to the effects of the vortices from the vortex generator on the static pressure tap readings. That is it could be a local phenomenon around the taps and the diffuser may not have any separation as reported in the experiment and confirmed by the computation.

To further verify the accuracy of the CFD code, in particular the boundary layer bleed model, we computed the axisymmetric case at the inlet design point Mach 2.5, where the second cone angle (18°) is 3.5° higher than the Mach 2.0 case. Fig. 5 displays the computational and experimental pressure distributions along the centerbody using the same mesh size as the baseline case. The shock location and intensity was again accurately predicted. The pressure distributions agreed very well in the subsonic diffuser without the deviation as shown in the Mach 2.0 case. For Mach 2.5 case, the experiment also reported no separation in that region.

At Mach 2 and zero angle of attack, the total pressure recovery predicted is 0.939 which is very accurate compared with the experimental value 0.938. However, the steady state distortion predicted is 0.165 and is significantly higher than the experimental value of 0.114. The reason for this outcome may be threefolds: 1) in the computation, there were no vortex generators which were used in the experiment to reduce the distortion by inhibiting flow separation; 2) the constant back pressure boundary condition might be

accurate to compute the averaged parameters on the compressor face such as the total pressure recovery, but might be not accurate to compute the distortion which depends on the maximum and minimum total pressure value; 3) the maximum and minimum total pressure determing the distortion from the experiment were from the limited total pressure probes on the exit cross-section. In the computation, they were from the mesh points which were much more finely distributed than the measurement probes on that cross-section.

Fig. 6 presents the Mach number contours of the 3D computation at zero angle of attack computed in the region of the throat and shows the shock wave structure. The normal shock is located in the middle of the bleed region. Fig. 7 displays the velocity vector field predicted using the current bleed boundary condition. The velocity going into the bleed slot is very large and is abruptly reduced by the normal shock wave. However, the bleed mass flow rate going into the bleed zone is uniform by assumption.

5.2 Prediction of Unstart Angle of Attack

After obtaining the flow at critical operation and zero angle of attack, computations of the flow field with different angles of attack were performed with the same back pressure as employed for zero angle of attack. In the experiment, the inlet at Mach 2 unstarted at an angle of attack equal to 1.3°. The final unstart angle of attack we obtained is 1.4° with the uncertainty $\pm 0.2°$. The $\pm 0.2°$ uncertainty is determined by verifying that the inlet remains started at 1.2° angle of attack and unstarts at 1.6°. We took $\pm 0.2°$ uncertainty range because it falls within the usual experimental measurement uncertainty.

Fig. 8 is the Mach number contours on the leeward and windward plane at different angles of attack. It is seen that the the oblique shock on the windward and leeward side becomes asymmetric about the axis when there is angle of attack. The inlet remains started at angle of attack 1.2° and becomes unstarted at angle of attack 1.6°. The figure also shows that a large separation was induced by the bowl shock in the forward portion of the inlet. The mechanism causing the inlet unstart due to angle of attack is analyzed in [23].

6 Conclusions

The NASA VDC HSCT inlet flow at Mach 2 with the angle of attack is simulated by using a 3D Navier-Stokes solver with Baldwin-Lomax algebraic turbulence model. An extrapolation uniform mass bleed boundary condition is suggested for the slot bleed and is proven to be quite robust and accurate. For zero angle of attack, critical operation flow is obtained with a back pressure that agrees with the experiment within 2.5%. The pressure distribution of the critical flow agrees very well with the experiment except in a portion of the subsonic diffuser where vortex generators were employed in the experiment. To further prove the robustness and accuracy of the bleed boundary conditions, the Mach 2.5 case with zero angle of attack was also computed. The pressure distribution is accurately predicted along the whole inlet including the region of the subsonic diffuser. The terminal shock location, intensity and total pressure recovery all agree well with the experiment. The steady state distortion on the compressor face is predicted 5% higher than the experiment. It may be mainly due to not simulating the vortex generators in the computation. The computed angle of attack for the inlet unstart is $1.4° \pm 0.2°$, which is in close agreement with the experimental value 1.3°. The mesh refinement computation confirms that the solution is converged based on the test for the axisymmetric flow with zero angle of attack.

7 Acknowledgments

This research is part of the HPCD (Hypercomputing and Design) project based at Rutgers University. The HPCD project is supported by the Defense Advanced Research Projects Agency of the Department of Defense through contract ARPA-DABT 63-93-C-0064 monitored by Dr. Bob Lucas. The contents of this paper

do not necessarily reflect the position of the United States government and official endorsement should not be inferred. UTRC supported the efforts of Martin Haas under its IR&D program. The authors would like to particularly thank Mr. J.D. Saunders at NASA Lewis Research Center for his helpful suggestions and providing his and other authors' reference papers. Special thanks are also extended to Dr. G. C. Paynter at Boeing, Dr. Tom I-P. Shih at Carnegie Mellon University, and Dr. J. W. Slater at ICOMP for their helpful discussion and providing their research papers. The authors also greatly appreciate the help of Dr. William D. McGrory at Aerosoft Inc. and Mr. Keith Miyake in the Dept of Computer Science of Rutgers University to incorporate the bleed boundary condition subroutine into GASP code.

References

[1] National Research Council, *Aeronautical Technologies for the Twenty-First Century,*. Committee on Aeronautical Technologies, National Research Council, National Academy Press, Washington, D.C., 1992.

[2] National Science and Technology Council, *Goals for a National Partnership in Aeronautics Research and Technology,*. Executive Office of the President of the United States, White House,, 1995.

[3] J. Saunders and T. Keith, "Results from Computational Analysis of a Mixed Compression Supersonic Inlet." AIAA Paper 91-2581, 1991.

[4] A. Hamed and T. Lehnig, "An Investigation of Oblique Shock/Boundary Layer Bleed Interaction." AIAA 90-1928, 1990.

[5] G. Cooper and J. Sirbaugh, "PARC Code: Theory and Usage." AEDC-TR-89-15, 1989.

[6] J. W. Slater, J. Chung, and G. L. Cole, "Computation of Unsteady Aeropropulsion Flows with Moving Geometry." Proceedings of 1st AFOSR Conference on Dynamic Motion CFD, Rutgers University, New Jersey, USA, June 3-5, 1996.

[7] D. Mayer and G. C. Paynter, "Prediction of Supersonic Inlet Unstart Caused by Freestream Disturbances," *AIAA Journal*, vol. 33, pp. 266–275, Feb. 1995.

[8] D. Mayer and G. C. Paynter, "Boundary conditions for Unsteady Supersonic Inlet Analyses," *AIAA Journal*, vol. 32, pp. 1200–1206, June, 1994.

[9] J. W. Slater, "Efficient Computation of Unsteady Planar Internal Viscous Flows with Moving Geometry." AIAA Paper 96-0113, 1996.

[10] M. D. Neaves and D. S. McRae, "Nnmerical investigations of axisymmetric and Three-Dimensional Supersonic Inlet Flow Dynamics Using a Solution Adaptive Mesh." Proceedings of 1st AFOSR Conference on Dynamic Motion CFD, Rutgers University, New Jersey, USA, June 3-5, 1996.

[11] B. D. Goble, S. King, J. Terry, and M. Schoop, "Inlet Hammershock Analysis Using a 3-D Unsteady Euler/Navier-Stokes Code." AIAA Paper 96-2547, 1996.

[12] D. N. Miller and B. R. Smith, "Time-Dependent CFD Analysis of Inlet Unstart." Proceedings of 1st AFOSR Conference on Dynamic Motion CFD, Rutgers University, New Jersey, USA, June 3-5, 1996.

[13] J. Vadyak, J. Hoffman, and A. R. Bishop, "Calculation of the Flow Field in Supersonic Mixed-Compression Inlets at Angle of Attack Using the Three-Dimensional Method of Characteristics with Discrete Shock Wave Fitting." NASA CR-135425, 1978.

[14] D. G. Howlett and L. Hunter, "A Study of a Supersonic Axisymmetric Spiked Inlet at Angle of Attack Using the 3-D Navier-Stokes Equations." AIAA Paper 86-0308, 1986.

[15] D. N. Bowditch, "Some Design Considerations for Supersonic Cruise Mixed Compression Inlets." NASA TM X-71460, 1973.

[16] J. F. Wasserbauer, R. J. Shaw, and H. E. Neumann, "Design of a Very-Low-Bleed Mach 2.5 Mixed-Compression Inlet with 45

Percent Internal Contraction." NASA TM X-3135, 1975.

[17] J. F. Wasserbauer, H. E. Neumann, and R. J. Shaw, "Distortion in a Full-Scale Bicone Inlet with Internal Focused Compression and 45 Percent Internal Contraction." NASA TM X-3133, 1974.

[18] J. F. Wasserbauer, H. E. Neumann, and R. J. Shaw, "Performance and Surge Limits of a TF30-P-3 Turbofan Engine/Axisymmetric Mixed-Compressino Inlet Propulsion Syetem at Mach 2.5." NASA TP 2461, 1985.

[19] "GASP v3 User's Manual." Aerosoft, Inc., May 1996.

[20] G. C. Zha, D. Smith, M. Schwabacher, K. Rasheed, A. Gelsey, and D. Knight, "High Performance Supersonic Missile Inlet Design Using Automated Optimization." AIAA Paper 96-4142, 1996.

[21] A. Harten, "High Resolution Schemes for Hyperbolic Conservation Laws," *Journal of Computational Physics*, vol. 49, pp. 357–353, 1983.

[22] W. Chyu, G. Howe, and T. I.-P. Shih, "Bleed Boundary Conditions for Numerically Simulated Mixed-Compression Sipersonic Inlet Flow," *Journal of Propulsion and Power*, vol. 8, pp. 862–868, July-Aug. 1992.

[23] G.-C. Zha, D. Knight, and D. Smith, "Numerical Investigations of HSCT Inlet Unstart Transient at Angle of Attack." in preparation.

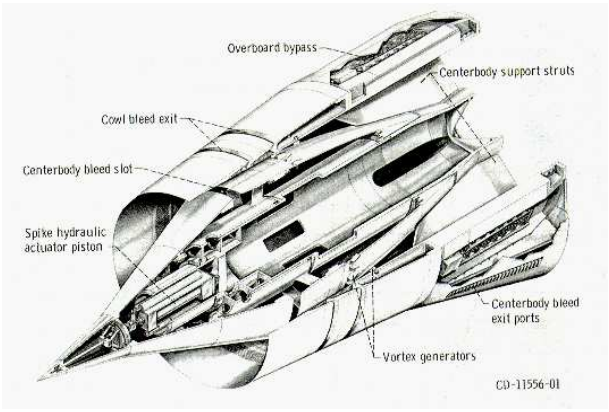

Figure 1: NASA VDC inlet cross section (from [16])

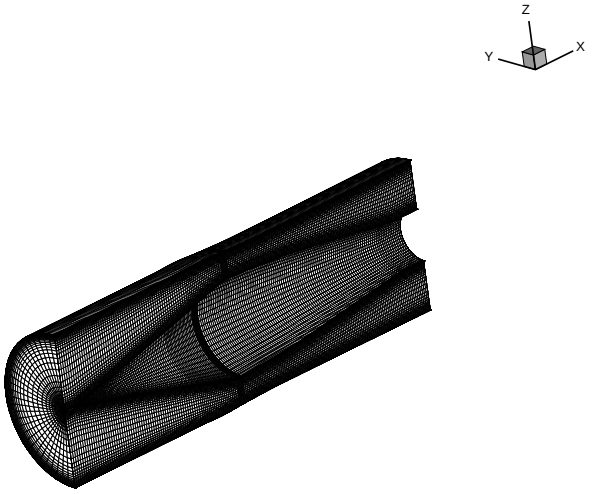

Figure 2: Geometry and mesh of the mixed compression inlet

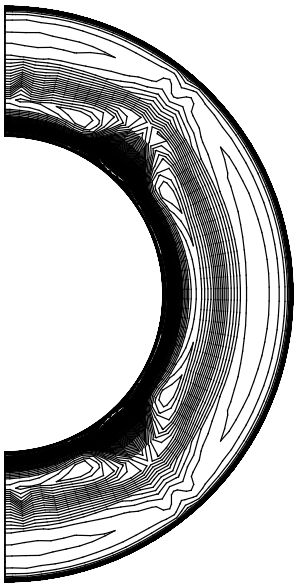

Figure 3: Mach contours at zero angle of attack upstream of the bleed region computed using the Roe scheme

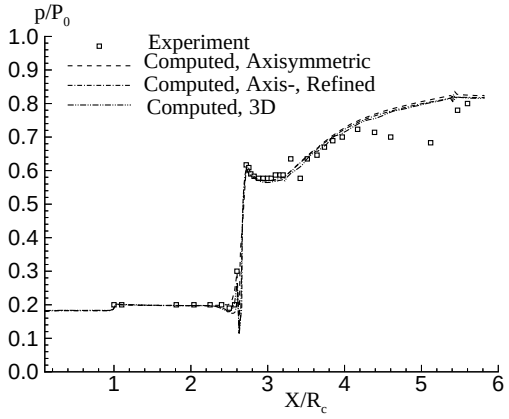

Figure 4: Pressure distributions along the center of the inlet for M=2.0 at $\alpha = 0°$

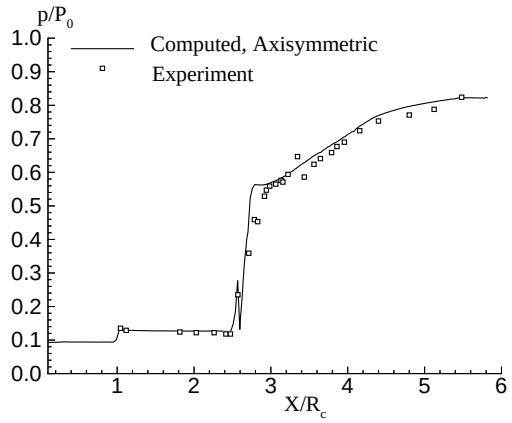

Figure 5: Pressure distributions along the center of the inlet for M=2.5 at $\alpha = 0°$

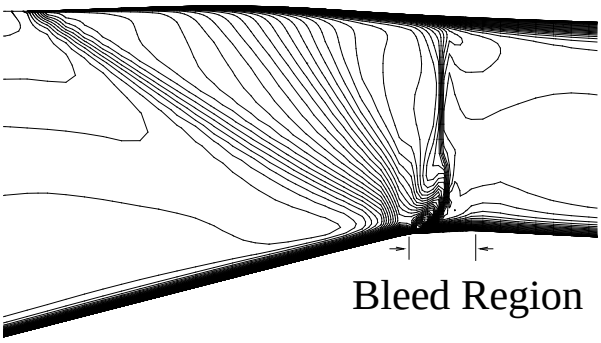

Figure 6: Mach contours in the region of the throat at critical operation for M=2.0 at $\alpha = 0°$

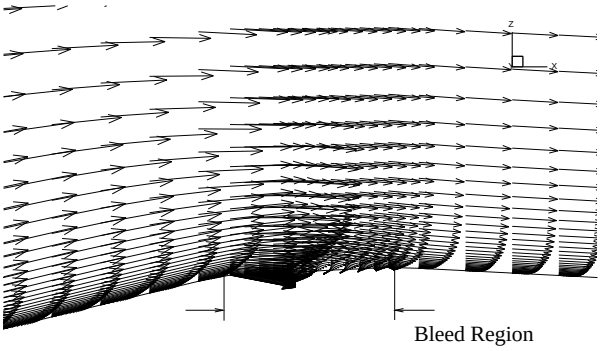

Figure 7: Velocity vector field in the bleed region for M=2.0 at $\alpha = 0°$

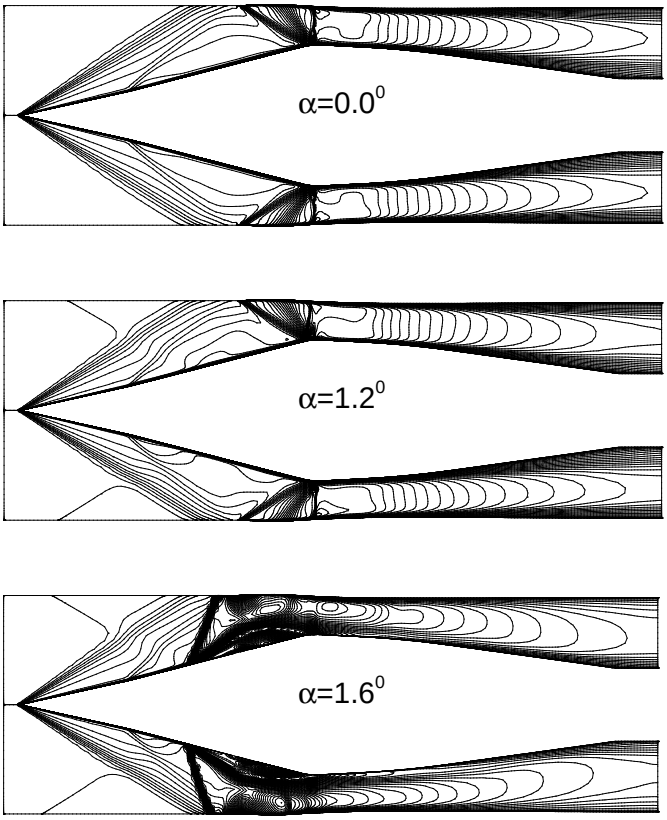

Figure 8: Mach number contours at different angle of attack showing inlet started at $\alpha = 0°$ and $\alpha = 1.2°$, and unstarted at $\alpha = 1.6°$